5. T. Hirano and T. J. Mitchison, *ibid.*, p. 449; Y. Saka *et al.*, *EMBO J.* **13**, 4938 (1994); A. V. Strunnikov, V. L. Larinov, D. Koshland, *J. Cell Biol.* **123**, 1635 (1993); N. Saitoh, I. G. Goldberg, E. R. Wood, W. C. Earnshaw, *ibid.* **127**, 303 (1994); A. V. Strunnikov, E. Hogan, D. Koshland, *Genes Dev.* **9**, 587 (1995); N. Saitoh, I. G. Goldberg, W. C. Earnshaw, *Bioessays* **17**, 759 (1995); T. Hirano, T. J. Mitchison, J. R. Swedlow, *Curr. Opin. Cell Biol.* **7**, 329 (1995).
6. A. M. Villeneuve and B. J. Meyer, *Cell* **48**, 25 (1987); *Genetics* **124**, 91 (1990); M. L. Nonet and B. J. Meyer, *Nature* **351**, 65 (1991).
7. L. Delong, J. D. Plenefisch, R. D. Klein, B. J. Meyer, *Genetics* **133**, 875 (1993).
8. C. Nusbaum and B. J. Meyer, *ibid.* **122**, 579 (1989).
9. J. Hodgkin, *Mol. Gen. Genet.* **192**, 452 (1983).
10. L. M. Miller, J. D. Plenefisch, L. P. Casson, B. J. Meyer, *Cell* **55**, 167 (1988).
11. N. R. Rhind, L. M. Miller, J. B. Kopczynski, B. J. Meyer, *ibid.* **80**, 71 (1995).
12. The *sdc-2* (*y74* or *y82*) and *sdc-3*(*y126*) null alleles cause such extensive XX-specific lethality and masculinization that mutants must be grown as *her-1*(*hv1y101*); *xol-1*(*y9*) *sdc* XO hermaphrodite strains. The XO-specific lethality caused by an *xol-1* mutation is suppressed by an *sdc* mutation, and the rescued XO animals are transformed into fertile hermaphrodites by a *her-1* mutation. The viable XO embryos and dying XX embryos were analyzed from this strain. Strains of *dpy-28*(*s939*) and *dpy-26*(*y65* or *n199*) null mutants did not require *her-1* because *dpy; xol-1* XO animals are hermaphrodites. We confirmed the results from the XO strains by examining anti–DPY-27 staining in a small sample of XX embryos from XX mutant mothers. The temperature-sensitive *dpy-30*(*y228*) and *dpy-28*(*y1*) XX mutants were grown as in (*20*). Because 30% of *sdc-3*(*y129*) XX mutants and all of the *sdc-1*(*n485*) and *dpy-21*(*e428*) mutants are viable, they were grown as XX strains.
13. P.-T. Chuang, J. D. Lieb, B. J. Meyer, unpublished data.
14. R. D. Klein and B. J. Meyer, *Cell* **72**, 349 (1993).
15. R. L. Kelley *et al.*, *ibid.* **81**, 867 (1995).
16. J. D. Lieb, E. E. Capowski, P. Meneely, B. J. Meyer, *Science* **274**, 1732 (1996).
17. Nuclei were prepared at 4°C; all buffers were supplemented with 1 mM dithiothreitol, 0.1% aprotinin, 0.2 mM phenylmethylsulfonyl fluoride (PMSF), 1 mM benzamidine, 1 mM sodium metabisulfite. Embryos (*14*) were resuspended in 3 ml of homogenization buffer [15 mM K Hepes (pH 7.6), 10 mM KCl, 5 mM $MgCl_2$, 0.1 mM EDTA, 350 mM sucrose] per wet gram and homogenized with 0.5-mm glass beads in a beadbeater (Biospec) for 7 min. The homogenate was filtered through 20-μm-diameter nylon mesh and centrifuged for 5 min at 900 rpm (SS-34 rotor). The supernatant was adjusted to 0.2% NP-40 and centrifuged for 15 min at 8000 rpm (SS-34 rotor). The pellet was resuspended in 5 ml of homogenization buffer per gram of starting embryos, transferred to a cold glass dounce (Kontes), dispersed with a type B pestle, and centrifuged for 15 min at 8000 rpm (SS-34 rotor). The pellet was resuspended in 30 ml of buffer A [15 mM K Hepes (pH 7.6), 60 mM KCl, 5 mM $MgCl_2$, 0.1 mM EDTA, 0.5 mM EGTA, 1.5 M sucrose] and dispersed as before. Nuclei were layered onto 7 ml of buffer A with 2.1 M sucrose and centrifuged for 2 hours at 24,500 rpm in an SW28 (Beckman) rotor. The pellet was washed and resuspended in homogenization buffer. For immunoprecipitations, 50 μg of affinity-purified anti–DPY-27 (specific for the first 409 amino acids) or anti–DPY-26 (specific for amino acids 739 to 1263) were added to 80 μl of protein A–Sepharose (Pharmacia) equilibrated in HEMK buffer [25 mM K Hepes (pH 7.6), 200 mM KCl, 12.5 mM $MgCl_2$, 0.1 mM EDTA, 10% glycerol, 0.2 mM PMSF, and 0.1% NP-40] and incubated for 3 hours at 4°C with rocking. Embryonic nuclei (100 to 300 mg) in HEMK buffer were sonicated and microcentrifuged at 14,000 rpm for 30 min at 4°C. The supernatant was preincubated with protein A–beads, centrifuged as above, and added to the antibody–protein A complexes. After 4 hours at 4°C with rocking, the antibody–protein A complexes were washed twice (15 min each) in HEMK buffer and twice in HEMK buffer with 400 mM KCl. The bound proteins were analyzed by SDS-PAGE.
18. Partial purification of a dosage compensation complex: Nuclei (1 g) were resuspended in HEMK buffer, sonicated, and microcentrifuged at 14,000 rpm for 30 min at 4°C. The supernatant was added to SP-Sepharose resin (1 ml) and incubated for 1 hour at 4°C with rocking. The protein complex was washed with HEMK buffer and eluted from a column with HEMK buffer containing 400 mM KCl. The eluate was adjusted to 200 mM KCl, added to Q-Sepharose resin, and the mixture treated as above. The fractions containing DPY-27 were immunoprecipitated with anti–DPY-26 or anti–DPY-27 as described (*17*). Resins (Pharmacia) were washed with HEMK buffer containing 400 mM KCl and then HEMK buffer before use.
19. H. E. Dawes, D. M. Lapidus, D. B. Berlin, B. J. Meyer, unpublished data.
20. D. R. Hsu, P.-T. Chuang, B. J. Meyer, *Development* **121**, 3323 (1995).
21. *dpy-30* probably exerts its effects on dosage compensation through regulation of *sdc-3*. *sdc-3* XX null mutants do not exhibit a sex-determination defect, even though *sdc-3* functions in sex determination (*7*). The sex determination defect is apparent in *sdc-3*(null); *xol-1* XO animals, which are males. In contrast, *xol-1* XO animals are hermaphrodites if also mutant in *dpy-26*, *dpy-27*, or *dpy-28*. *dpy-30* mutations behave like *sdc-3* null mutations in that extensive masculinization is apparent only in the *dpy-30; xol-1* XO animals (*3*). For comparison, *sdc-2* XX mutants are very masculinized.
22. We thank T. Cline, R. Tjian, G. Garriga, J. Rine, M. Botchan, I. Carmi, T. Davis, and H. Dawes for critical comments on the manuscript; C. Akerib for strain construction; and R. Kamakaka, H. Beckmann, and S. Lichtsteiner for advice. Supported by U.S. Public Health Service (USPHS) grant GM30702 and American Cancer Society grant DB-5B (to B.J.M.) and USPHS grant T32 GM07127 (to J.D.L.).

26 August 1996; accepted 1 October 1996

Molecular Mimicry of Human Cytokine and Cytokine Response Pathway Genes by KSHV

Patrick S. Moore, Chris Boshoff, Robin A. Weiss, Yuan Chang*

Four virus proteins similar to two human macrophage inflammatory protein (MIP) chemokines, interleukin-6 (IL-6), and interferon regulatory factor (IRF) are encoded by the Kaposi's sarcoma–associated herpesvirus (KSHV) genome. vIL-6 was functional in B9 proliferation assays and primarily expressed in KSHV-infected hematopoietic cells rather than KS lesions. HIV-1 transmission studies showed that vMIP-I is similar to human MIP chemokines in its ability to inhibit replication of HIV-1 strains dependent on the CCR5 co-receptor. These viral genes may form part of the response to host defenses contributing to virus-induced neoplasia and may have relevance to KSHV and HIV-I interactions.

Kaposi's sarcoma–associated herpesvirus (KSHV) is a gammaherpesvirus (*1*, *2*) related to Epstein-Barr virus (EBV) and herpesvirus saimiri (HVS). It is present in nearly all KS lesions including the various types of HIV-related and HIV-unrelated KS (*1*, *3*, *4*). Moreover, viral DNA is localized to KS tumors (*1*, *4*, *5*) and serologic studies show that KSHV is specifically associated with KS (*2*, *6*–*8*). Taken together, these studies indicate that KSHV is the probable infectious agent precipitating KS in patients with and without HIV (*9*). Related lymphoproliferative disorders, which can occur in patients with KS [such as body-cavity-based/primary effusion lymphoma (PEL), a rare B cell lymphoma, and some forms of Castleman's disease] are also associated with KSHV infection (*10*).

To identify viral genes in the KSHV genome, genomic sequencing (*11*) was performed with Supercos-1 and Lambda FIX II genomic libraries from BC-1, a non-Hodgkin's lymphoma cell line stably infected with both KSHV and EBV (*12*). The KSHV DNA fragments KS330Bam and KS631Bam (*1*) were used as hybridization starting points for mapping and bi-directional sequencing (*11*). Open reading frame (ORF) analysis (*13*) of the Z6 cosmid sequence identified two separate potential coding regions (ORFs K4 and K6) with sequence similarity to β-chemokines and a third potential coding region (ORF K2) similar to human interleukin-6 (huIL-6); a fourth potential coding region (ORF K9) is present in the Z8 cosmid insert sequence with sequence similarity to interferon regulatory factor (IRF) proteins (Fig. 1). None of these KSHV genes are similar to other known viral genes (*14*) and the predicted proteins were named without reference to their potential in vivo functional properties.

The 289-bp ORF of the K6 gene encodes a 10.5-kD predicted protein (vMIP-I) with 37.9% amino acid identity (71% similarity) to huMIP-1α and slightly greater differences with other β-chemokines (Fig. 1A). ORF K4 also encodes a predicted 10.5-kD protein (vMIP-II), similar in sequence and amino acid hydrophobicity

P. S. Moore, School of Public Health and Y. Chang, Department of Pathology, Columbia University, New York, NY 10032, USA.
C. Boshoff and R. A. Weiss, Chester Beatty Laboratories, Institute of Cancer Research, London SW3 6JB, UK.
*To whom correspondence should be addressed.

profile to vMIP-I. The two KSHV-encoded genes that are similar to β-chemokines are separated from each other on the KSHV genome by 5.5 kb of intervening sequence containing at least four potential ORFs (*11*). Both hypothetical proteins have conserved β-chemokine motifs (Fig. 1A, residues 17 to 55) that include a characteristic C-C dicysteine dimer (Fig. 1A, residues 36 to 37), and have near sequence identity to human MIP-1α at residues 56 to 84. However, the two proteins show only 49.0% amino acid identity to each other and are markedly divergent at the nucleotide level, indicating that this duplication is not a cloning artifact. The two viral proteins are more closely related to each other phylogenetically than to huMIP-1α, huMIP-1β, or huRANTES, suggesting that they arose by gene duplication rather than independent acquisition from the host genome (*15*). The reason for this double gene dosage in the viral genome is unknown.

The KSHV ORF K2 (Fig. 1B) encodes an IL-6–like protein of 204 amino acids (23.4 kD). It contains a hydrophobic 19–amino acid secretory signaling peptide having 24.8% amino acid identity and 62.2% similarity to the human protein. The vIL-6 also has a conserved sequence characteristic of IL-6–like interleukins (residues 101 to 125 of the gapped protein) as well as four conserved cysteines that are present in IL-6 proteins (gapped alignment residue positions 72, 78, 101, and 111 in Fig. 1B). Potential N-linked glycosylation sites in the vIL-6 sequence are present at gapped positions 96 and 107 in Fig. 1C. The 449–

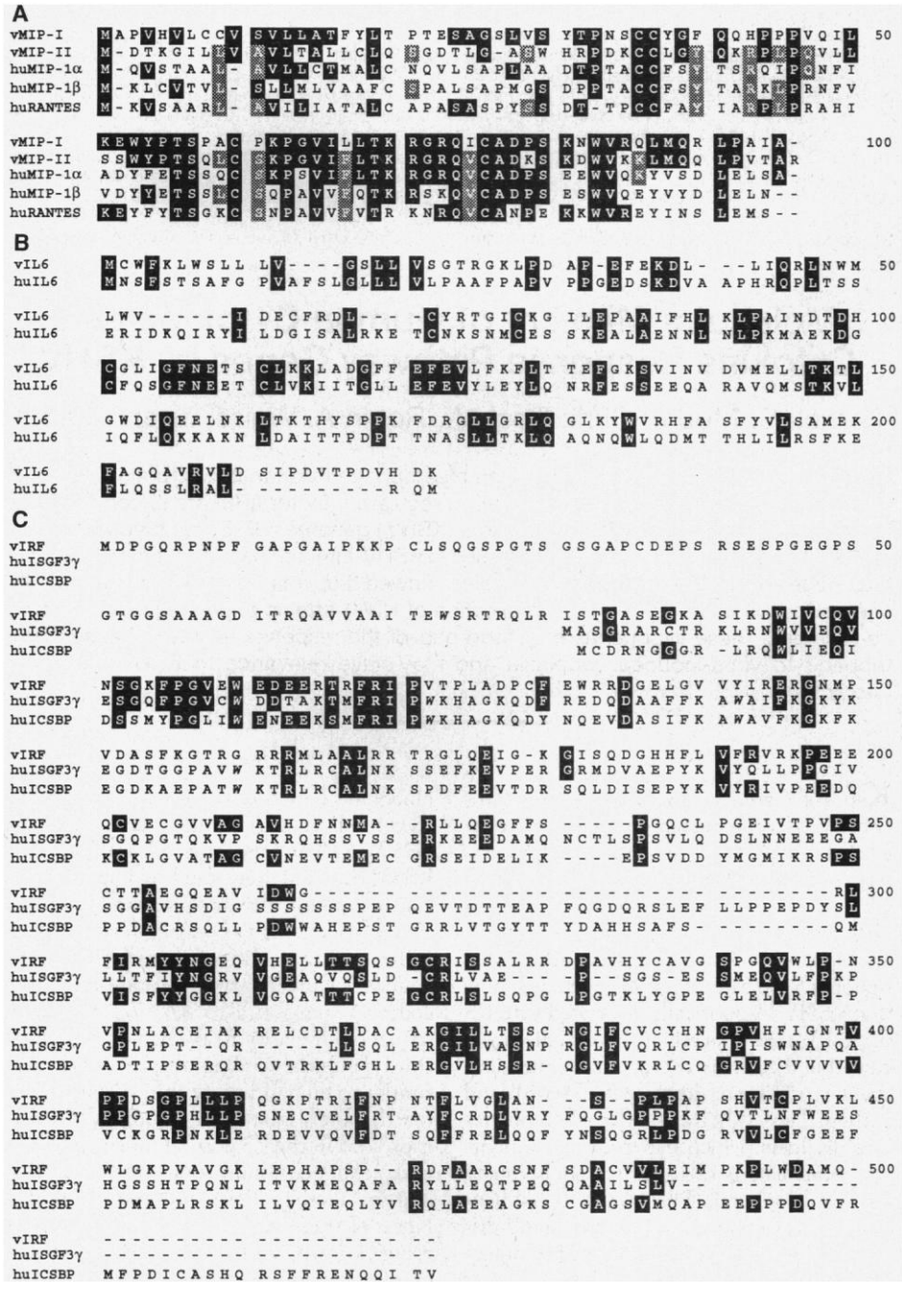

Fig. 1. CLUSTAL W alignments of KSHV-encoded, hypothetical protein sequences to corresponding human protein sequences. (**A**) Two KSHV MIP-like genes (vMIP-I and vMIP-II) are compared to human MIP-1α, MIP-1β, and RANTES (amino acid identity to vMIP-I indicated by black reverse shading, to vMIP-II alone by gray reverse shading; the C-C dimer motif is italicized). The KSHV MIP genes encode 24– and 23–amino acid, NH_2-terminus hydrophobic secretory leader sequences, respectively, that are relatively poorly conserved (vMIP-I also has a second C-C dimer in the hydrophobic leader sequence without similarity to the chemokine dicysteine motif). Potential O-linked glycosylation sites for vMIP-I (gapped positions 22 and 27) are not present in vMIP-II, which has only one predicted serine glycosylation site (position 51) not found in vMIP-I. (**B**) Alignment of the KSHV vIL-6 to human IL-6. (**C**) Alignment of the KSHV vIRF protein to human ICSBP and ISGF3γ with the putative ICS-binding tryptophans (W) for ICSBP and ISGF3γ in italics.

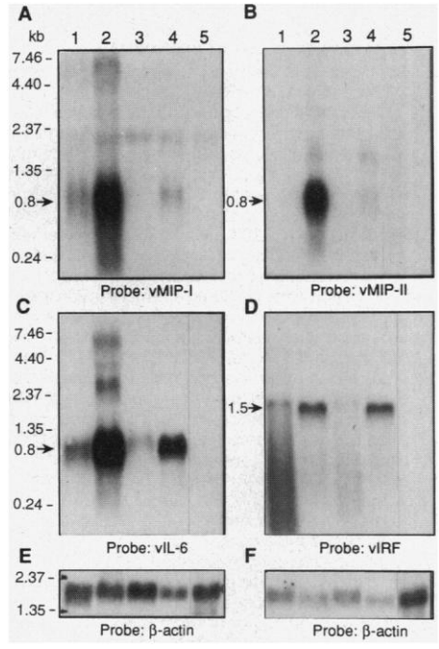

Fig. 2. Expression of KSHV genes in infected cells in the presence or absence of TPA induction. Northern hybridization was performed on total RNA extracted from BCP-1 (lanes 1 and 2) and BC-1 cells (lanes 3 and 4) prior to and after a 48-hour incubation with TPA, respectively, and on control P3HR1 cells (lane 5) after TPA incubation. All four genes (**A**, vMIP-I; **B**, vMIP-II; **C**, vIL-6; and **D**, vIRF) are TPA-inducible. Representative hybridizations to a human β-actin probe (**E** and **F**) demonstrate comparable loading of RNA.

amino acid KSHV vIRF protein encoded by ORF K9 has lower overall amino acid identity (approximately 13%) to its human cellular counterparts than either of the vMIPs or the vIL-6, but has a conserved region derived from the IRF family of proteins (Fig. 1C, gapped residues 88 to 121). This region includes the tryptophan-rich DNA binding domain for IRF, although only two of four tryptophans thought to be involved in DNA binding are positionally conserved. It is preceded by an 87–amino acid peptide with a hydrophilic NH_2-terminus having little apparent IRF similarity; the COOH-terminus also has low amino acid similarity to the IRF family transactivator/repressor region.

The four KSHV proteins that resemble members of cell signaling pathways show similar patterns of expression in virus-infected lymphocyte cell lines by Northern blotting (*16*). Whole RNA was extracted from BCP-1 [a cell line infected with KSHV alone (*17*)] and BC-1 [EBV, KSHV coinfected (*12*)] with or without pretreatment with 12-O-tetradecanoylphorbol-13-acetate (TPA, 20 ng/ml, Sigma, St. Louis, Missouri) for 48 hours. Although constitutive expression of these genes was variable between the two cell lines, expression of all four gene transcripts increased in BCP-1 and BC-1 cells after TPA induction (Fig. 2, A to D). This pattern is consistent with expression occurring primarily during virus replication in the lytic phase. Examination of viral terminal repeat sequences of BCP-1 and BC-1 demonstrates that a small amount of lytic replication occurs in BCP-1 but not BC-1 in the absence of TPA induction (*11*), and both cell lines can be induced to express lytic-phase genes by TPA treatment despite repression of DNA replication in BC-1 (*18*). A lower level of expression during latent replication is seen, particularly for vIL-6 (Fig. 2C) and vIRF (Fig. 2D), as these transcripts were detectable in the absence of TPA induction in BC-1 cells, which are under tight latency control. Although cytokine dysregulation has been proposed to cause KS (*19*), spindle cell lines used for in vitro studies over the past decade are uniformly uninfected with KSHV (*20*). To determine if KS spindle cells cultured in vitro retain defective or partial virus sequences that include these genes, DNA was extracted from four KS spindle cell lines (KS-2, KS-10, KS-13, and KS-22) and amplified by the polymerase chain reaction for vMIP-I, vMIP-II, vIL-6, and vIRF sequences (*16*). None of the DNA samples from spindle cells was positive for any of the four genes.

The vIL-6 was examined in more detail by bioassays and antibody localization studies to determine whether it is functionally conserved. Recombinant vIL-6 (rvIL-6) (*21*) was specifically recognized by antipeptide antibodies that did not cross-react with huIL-6 (Fig. 3) (*22*). The vIL-6 was produced constitutively in BCP-1 cells and increased markedly after 48 hours of TPA induction, consistent with Northern hybridization experiments. The BC-1 cell line coinfected with both KSHV and EBV only showed vIL-6 protein expression after TPA induction and control EBV-infected P3HR1 cells were negative for vIL-6 expression (Fig. 3A). Multiple high molecular weight bands present after TPA induction (21 to 25 kD) may represent precursor forms of the protein. Despite regions of sequence dissimilarity between huIL-6 and vIL-6, the viral interleukin has biologic activity in functional bioassays with the mouse plasmacytoma cell line B9, which undergoes paracrine-dependent apoptosis in the absence of IL-6 (*23*). COS7 supernatants from the forward construct (rvIL-6) supported B9 cell proliferation measured by ^{3}H-thymidine uptake, indicating that vIL-6 can substitute for cellular IL-6 in preventing B9 apoptosis (Fig. 3B). Proliferation of B9 cells in the presence of vIL-6 was dose-dependent, with the unconcentrated supernatant from the experiment shown in Fig. 4 having biologic activity equivalent to approximately 20 picograms per milliliter of huIL-6.

Forty-three percent of noninduced BCP-1 cells (Fig. 4A) had intracellular cytoplasmic vIL-6 immunostaining (*24*) suggestive of constitutive virus protein expres-

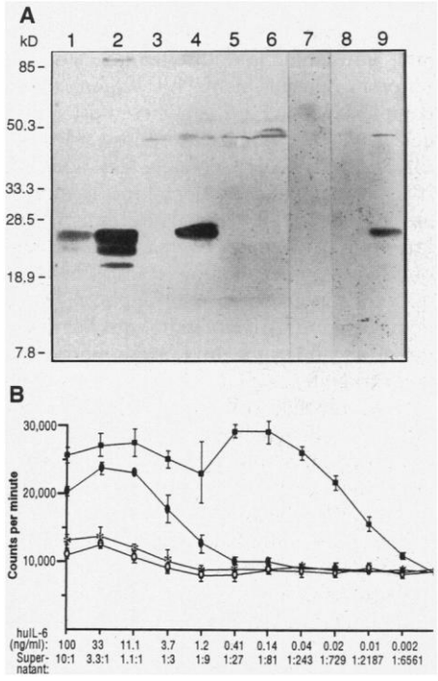

Fig. 3. (**A**) Immunoblot of rabbit antipeptide antibodies generated from the predicted amino acid sequences of vIL-6 [THYSPPKFDR and PDVTPDVHDR (*41*)] against cell lysates of BCP-1 (lane 1), BCP-1 plus TPA (lane 2), BC-1 (lane 3), BC-1 plus TPA (lane 4), P3HR1 (lane 5), P3HR1 with TPA (lane 6), 1 μg human rIL-6 (lane 7), and concentrated COS7 r6-LIv (lane 8) and rvIL-6 supernatants (lane 9). Preimmune sera from immunized rabbits did not react on immunoblotting to any of the preparations. (**B**) Dose-response curves for ^{3}H-thymidine uptake in IL-6–dependent B9 cells with serial dilutions of rhuIL-6 (filled squares) and COS7 supernatants of rvIL-6 (filled circles), r6-LIv (asterisks) or control LacZ (open circles) pMET7 transfections. Undiluted rvIL-6 supernatants from this transfection lot showed similar B9 proliferation activity to huIL-6 >0.02 ng/ml whereas the reverse construct (r6-LIv) and the LacZ control showed no increased ability to induce B9 proliferation. Concentrated supernatants at greater than 1:1 dilution may have increased activity due to concentration of COS7 conditioning factors.

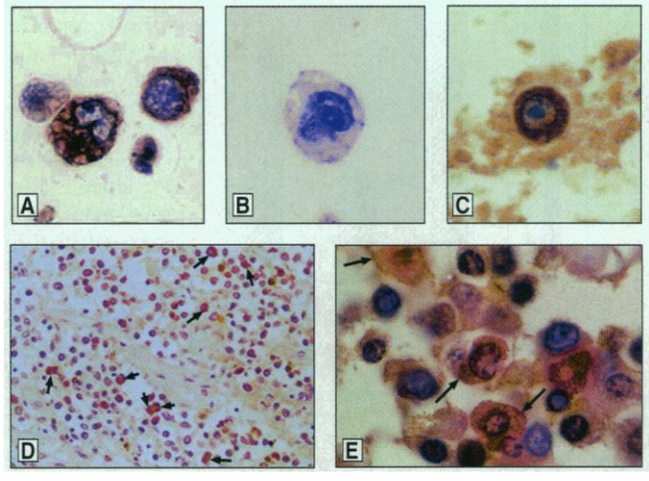

Fig. 4. Antibody localization studies of cultured infected cells and patient tissues indicate that vIL-6 is primarily expressed in infected hematopoietic cells. Rabbit anti–vIL-6 peptide antibody reactivity localized with goat-antirabbit immunoglobulin-peroxidase conjugate (brown) plus hematoxylin counterstaining (blue) at 60× final magnification. KSHV-infected cell line BCP-1 (**A**), EBV-infected cell line P3HR1 (**B**), pelleted lymphoma cells from a non-AIDS, EBV-negative PEL (**C**). Widespread positivity (Vector-Red staining) is also seen at 12× final magnification in cells from a lymph node of an AIDS-KS patient (**D**). Arrows only indicate the most prominently staining cells; nuclei counterstained with hematoxylin. Colocalization (**E**) with CD20 (brown, arrows) and vIL-6 (red) in an AIDS-KS patient's lymph node (60×).

sion in cultured infected cells (*25*), whereas no specific immunoreactive staining was present in uninfected control P3HR1 cells (Fig. 4B). The vIL-6 protein was rarely detected in KS tissues and only one of eight KS lesions examined showed clear, specific vIL-6 immunostaining (in less than 2% of cells). The specificity of this low positivity rate was confirmed with preimmune sera and neutralization with excess vIL-6 peptides (*25*). These rare, vIL-6–producing cells in the KS lesion are positive for either CD34, an endothelial cell marker, or CD45, a pan-hematopoietic cell marker, demonstrating that both infected endothelial and hematopoietic cells in KS lesions can produce vIL-6. It is possible that these vIL-6–positive cells are entering lytic phase replication, which has been shown to occur with the KSHV T1.1 lytic phase RNA probe (*26*). In contrast, well over half (65%) of ascitic lymphoma cells pelleted from an HIV-negative PEL (*17*) are strongly positive for vIL-6 (Fig. 4C) and express the plasma cell marker EMA, indicating that either most PEL cells in vivo are replicating a lytic form of KSHV or that latently infected PEL cells can express high levels of vIL-6. No specific vIL-6 staining occurred with any control tissues examined including normal skin, tonsillar tissue, multiple myeloma, or angiosarcoma when either preimmune or post-immune rabbit anti–vIL-6 were used.

Virus dissemination to non-KS tissues was examined in lymph node tissue from a patient with AIDS-KS who did not develop PEL. Numerous hematopoietic cells staining with vIL-6 antibody were present in this lymph node (Fig. 4D), which was free of KS microscopically. The vIL-6–positive lymph node cells were present in relatively B cell–rich areas and some expressed the B cell surface antigen CD20 (Fig. 4E), but unlike PEL cells did not express EMA surface antigen (*12*). No colocalization of vIL-6 positivity with the T cell surface antigen CD3 or the macrophage antigen CD68 was detected, although phagocytosis of vIL-6 immunopositive cells by macrophages was frequently observed.

Members of the MIP/RANTES family of C-C chemokines prevent nonsyncytia-inducing (NSI) HIV-1 entry and replication by binding to the CCR5 chemokine receptor, which also is the HIV-1 co-receptor (*27*). To investigate whether vMIP-I can inhibit NSI HIV-1 entry, human $CD4^+$/cat kidney cells (CCC/CD4) were transiently transfected with plasmids expressing human CCR5 and vMIP-I or its reverse construct I-PIMv (*28*). These cells were infected with either M23 or SF162 primary HIV-1 isolates which are NSI and are known to use CCR5 as a co-receptor (*29*). Alternatively, they were infected with the HIV-2 variant ROD/B, which can infect $CD4^+$ CCC cells in the absence of human CCR5 (*28, 29*). Virus entry and replication were assayed by immunostaining for retroviral antigen production (Fig. 5). Cotransfection of vMIP-I reduced generation of NSI HIV-1–containing foci to less than half that of the reverse-construct negative control, but had no effect on ROD/B HIV-2 replication. This suggests that vMIP-I is functional in binding CCR5 and may contribute to interactions between KSHV and HIV-1.

Molecular piracy of host cell genes is a newly recognized feature of some DNA viruses, particularly herpesviruses and poxviruses (*14, 30*). In addition to vMIP-I, vMIP-II, vIL-6 and vIRF, KSHV also encodes genes similar to *bcl-2* (ORF 16), cyclin D (ORF 72), complement-binding proteins similar to CD21/CR2 (ORF 4), an NCAM-like adhesion protein (ORF K14), and an IL-8–like receptor (ORF 74) (*11, 31*). There is a striking correspondence between genes encoded by KSHV and human genes induced after EBV infection. EBV also encodes a Bcl-2–like protein (BHRF1) and induces human Bcl-2, complement-binding CR-2, cyclin D, IL-6, adhesion molecules, and the IL-8R–like EBI1 protein (*32, 33*). KSHV lacks genes with sequence similarity to EBV EBNA-LMP genes (*11*), which are largely responsible for induction of these cellular genes. Therefore, both viruses appear to modify the same cell regulatory and signaling pathways, but use different strategies to achieve these effects.

Identification of these viral genes leads to speculation about their potential roles in protecting against cellular antiviral responses. Cellular responses to virus infection commonly include cell cycle arrest, induction of apoptosis, and enhancement of cell-mediated immunity; many of these responses may be mediated through p53, which is commonly inactivated by DNA tumor viruses (*34*). The KSHV-encoded cyclin can functionally substitute for D-type cyclins in preventing pRB-mediated cell cycle arrest but similar to adenovirus EIA can induce apoptosis in cells with wild-type p53 (*31*). The huIL-6 inhibits apoptosis in myeloma cell lines which can be antagonized by interferons (*35*) and vIL-6 may play a similar role in infected B cells. KSHV-encoded vIRF and vbcl-2 may also contribute to prevention of host-cell–mediated apoptosis after virus infection. Interference with interferon-induced major histocompatibility complex (MHC) antigen presentation and cell-mediated immune response (*36*) by vIRF are additional possible functions for this protein. The β-chemokine homologs are more difficult to evaluate as it is unknown whether they have agonist or antagonist signal transduction roles. Their sequence conservation and duplicate gene dosage are indicative of important but as yet unknown functions in KSHV replication and survival.

Uncontrolled cell growth from dysregulation of cell-signaling pathways is an obvious potential by-product of this virus strategy. Given the paucity of cells expressing vIL-6 in KS lesions, it is unlikely that vIL-6 significantly contributes to KS cell neoplasia. KSHV induction of huIL6, however, with subsequent induction of vascular endothelial growth factor–mediated angiogenesis (*37*), is a possibility. The vIL-6 could potentially contribute to the pathogenesis of KSHV-related lymphoproliferative disorders such as PEL or the plasma cell variant of Castleman's disease. Apoptosis of multiple myeloma cells is prevented by huIL-6 (*35*), which is reflected by our studies of vIL-6 on B9 cell proliferation. The autocrine dependence on IL-6 and enhanced tumorigenicity of EBV-infected lymphocytes in the presence of IL-6 (*33, 38*) may be a similar manifestation of this requirement to overcome virus activation of apoptotic pathways in the host cell. The functional activity of vIRF is currently unknown, but a related member of this signal transduction protein family (IRF) has transforming capacity (*39*). The oncogenic potential of cellular cyclin and Bcl-2 overexpression is well established and these functional, virus-encoded homologs may also contribute to KSHV-related neoplasia.

KSHV vMIP-I inhibits NSI HIV-1 replication in vitro, but the clinical impor-

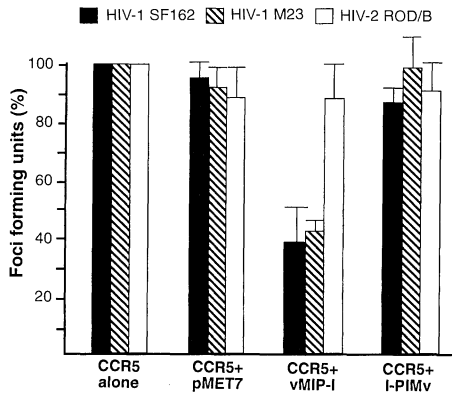

Fig. 5. CCC/CD4 cell infection by primary NSI SF162 and M23 HIV-1 strains and HIV-2 strain ROD/B in the presence or absence of vMIP-I. CCC/CD4 cells were transiently cotransfected with CCR5 alone, CCR5 plus empty pMET7 vector, CCR5 plus vMIP-I in pMET7 vector, or CCR5 plus the reverse orientation I-PIMv. The results after 72 hours of incubation with each retrovirus are expressed as a percentage of the foci forming units for cells transfected with CCR5 alone.

tance of this finding is unknown. Studies from early in the AIDS epidemic indicate that survival is longer for AIDS-KS patients than for other AIDS patients. Among U.S. AIDS patients, 93% of long-term survivors living >3 years with AIDS had KS compared to only 28% of AIDS patients living 2 years or less (*40*). This may be due to KS occurring at relatively high $CD4^+$ counts and competing mortality from other AIDS-defining conditions. Recent surveillance data indicates that the epidemiology of AIDS-KS is changing as the AIDS epidemic progresses (*40*). Additional studies will be needed to determine what effects, if any, KSHV-encoded cytokines have on HIV replication in vivo.

REFERENCES AND NOTES

1. Y. Chang *et al.*, *Science* **265**, 1865 (1994).
2. P. S. Moore *et al.*, *Virology* **70**, 549 (1996).
3. C. Boshoff *et al.*, *Lancet* **345**, 1043 (1995); P. S. Moore and Y. Chang, *N. Engl. J. Med.* **332**, 1181 (1996); M. Schalling *et al.*, *Nature Med.* **1**, 707 (1995); Y. Chang *et al.*, *Archiv. Int. Med.* **156**, 202 (1996).
4. N. Dupin *et al.*, *Lancet* **345**, 761 (1995).
5. C. Boshoff *et al.*, *Nature Med.* **1**, 1274 (1995); W. Zhong, H. Wang, B. Herndier, D. Ganem, *Proc. Natl. Acad. Sci. U.S.A.* **93**, 6641 (1996).
6. G. Miller *et al.*, *N. Engl. J. Med.* **334**, 1292 (1996); D. H. Kedes *et al.*, *Nature Med.* **2**, 918 (1996); G. R. Simpson *et al.*, *Lancet* **348**, 1133 (1996); E. T. Lennette, B. J. Blackbourne, J. A. Levy, *ibid.*, p. 858.
7. S.-J. Gao *et al.*, *Nature Med.* **2**, 925 (1996).
8. S.-J. Gao *et al.*, *N. Engl. J. Med.* **335**, 233 (1996).
9. V. Beral, *Cancer Surveys* **10**, 5 (1991); T. A. Peterman, H. W. Jaffe, V. Beral, *AIDS* **7**, 605 (1993); R. A. Weiss, *Nature Med.* **2**, 277 (1996); J. J. O'Leary, *ibid.*, p. 862.
10. E. Cesarman, Y. Chang, P. S. Moore, J. W. Said, D. M. Knowles, *N. Engl. J. Med.* **332**, 1186 (1995); J. Soulier *et al.*, *Blood* **86**, 1276 (1995); A. Gessain *et al.*, *ibid.* **87**, 414 (1996); M. Corbellino *et al.*, *Clin. Infect. Dis.* **22**, 1120 (1996).
11. Genomic inserts were randomly sheared, cloned into M13mp18, and sequenced to greater than 12-fold average redundancy with complete bidirectional sequencing. Details of KSHV genomic sequencing are reported in J. J. Russo *et al.*, *Proc. Natl. Acad. Sci. U.S.A.* **93**, 14862 (1996). The descriptive nomenclature of KSHV genes is based on the naming system derived for herpesvirus saimiri [J.-C. Albrecht *et al.*, *J. Virol.* **66**, 5047 (1992)].
12. E. Cesarman *et al.*, *Blood* **86**, 2708 (1995).
13. Assembled sequence contigs were analyzed with MacVector (IBI-Kodak, Rochester, NY) for potential open reading frames greater than 25 amino acid residues and analyzed with BLASTX and BEAUTY-BLASTX [S. F. Altschul, W. Gish, W. Miller, E. W. Myers, D. J. Lipman, *J. Mol. Biol.* **215**, 403 (1990); K. C. Worley, B. A. Wiese, R. F. Smith, *Genome Res.* **5**, 173 (1995); http://dot.imgen.bcm.tmc.edu:9331/seq-search/nucleic_acid-search.html]. Homologous proteins were aligned to the four proteins as follows (name, species, sequence bank accession number, smallest sum Poisson distribution probability score): *vMIP-I*: LD78 (MIP-1α) (human, gi127077, $P = 9.8 \times e^{-22}$), MIP-1α (*Rattus*, gi790633, $P = 3.3 \times e^{-20}$), MIP-1α (*Mus*, gi127079, $P = 1.7 \times e^{-19}$), MIP-1β (*Mus*, gi1346534, $P = 7.8 \times e^{-18}$). *vMIP-II*: LD78 (MIP-1α) (human, gi127077, $P = 7.1 \times e^{-23}$); MIP-1α (*Mus*, gi127079, $P = 8.9 \times e^{-21}$), MIP-1α (*Rattus*, gi790633, $P = 1.2 \times e^{-20}$), MIP-1β (Mus, gi1346534, $P = 3.8 \times e^{-20}$). *vIL-6*: 26-kD protein (IL-6) (human, gi23835, $P = 7.2 \times e^{-17}$); IL-6 (*Macaca*, gi514386, $P = 1.6 \times e^{-16}$). *vIRF*: ICSBP (*Gallus*, gi662355, $P = 1.1 \times e^{-11}$); ICSBP (*Mus*, spp23611, $P = 1.0 \times e^{-10}$); lymphoid specific interferon regulatory factor (*Mus*, gi972949, $P = 2.0 \times e^{-10}$); ISGF3 (*Mus*, gi1263310, $P = 8.1 \times e^{-10}$); IRF4 (human, gi1272477, $P = 1.0 \times e^{-9}$); ISGF3-γ (human, spQ00978, $3.9 \times e^{-9}$); ICSBP (human, spQ02556, $P = 2.3 \times e^{-8}$).
14. A hypothetical protein with conserved cysteine motifs similar to β-chemokine motif signatures has recently been reported in the molluscum contagiosum virus (MCV) genome [T. G. Senkevich *et al.*, *Science* **273**, 813 (1996)]. Neither vMIP-I or vMIP-II have significant similarity to the MCV protein.
15. Amino acid sequences were aligned by CLUSTAL W [J. D. Thompson, D. G. Higgins, T. J. Gibson, *Nucl. Acids Res.* **22**, 4673 (1994)] and compared by means of PAUP 3.1.1. Both rooted and unrooted bootstrap comparisons produced phylogenetic trees having all 100 bootstrap replicates with viral homologs being less divergent from each other than from the human homologs. The authors thank S. Olsen for performing the parsimony analysis.
16. Northern blotting was performed under standard conditions with random-labeled probes (*1*) derived from PCR products for the following primer sets: vMIP-I: 5′-AGC ATA TAA GGA ACT CGG CGT TAC-3′, 5′-GGT AGA TAA ATC CCC CCC CTT TG-3′; vMIP-II: 5′-TGC ATC AGC TTC TTC ACC CAG-3′, 5′-TGC TGT CTC GGT TAC CAG AAA AG-3′; vIL-6: 5′-TCA CGT CGC TCT TTA CTT ATC GTG-3′, 5′-CGC CCT TCA GTG AGA CTT CGT AAC-3′; vIRF: 5′-CTT GCG ATG AAC CAT CCA GG-3′, 5′-ACA ACA CCC AAT TCC CCG TC-3′ on total cell RNA extracted with RNAzol according to manufacturer's instructions (TelTest Inc., Friendswood, TX) and 10 μg of total RNA was loaded in each lane. BCP-1, BC-1, and P3HR1 were maintained in culture conditions and induced with TPA as described (*8*). PCR amplification for these viral genes was performed with the vMIP-I, vMIP-II, vIL-6, and vIRF primer sets in 35 amplification cycles and compared to dilutions of whole BC-1 DNA as a positive control; PCR conditions were as described [P. S. Moore and Y. Chang, *N. Engl. J. Med.* **332**, 1181 (1996)]. DNA from KS spindle cell lines used for these experiments was described in M. Dictor, E. Rambech, D. Way, M. Witte, N. Bendsöe, *Am. J. Pathol.* **148**, 2009 (1996) and kindly provided by M. Dictor, D. Way, and M. Witte. Amplifiability of DNA samples was confirmed with human HLA-DQ α and pyruvate dehydrogenase primers.
17. J. A. Strauchen *et al.*, *Ann. Intern. Med.* **125**, 822 (1996). Peripheral lymphocytes from the patient whose PEL tumor is shown in Fig. 4C were used to originate the BCP-1 cell line (*7*).
18. O. Flore, S.-J. Gao, P. S. Moore, unpublished observation.
19. B. Ensoli *et al.*, *Nature* **371**, 674 (1994); S. A. Miles, *Cancer Treatment Res.* **63**, 129 (1992).
20. J. A. Ambroziak *et al.*, *Science* **268**, 582 (1995); C. Lebbé *et al.*, *Lancet* **345**, 1180 (1995); M. Dictor, E. Rambech, D. Way, M. Witte, N. Bendsöe, *Am. J. Pathol.* **148**, 2009 (1996); L. Flamand, R. A. Zeman, J. L. Bryant, Y. Lunardi-Iskandar, R. C. Gallo, *J. AIDS Hum. Retrovirol.* **15**, 194 (1996).
21. The vIL-6 was cloned from a 695-bp polymerase chain reaction product with the primer set described (*16*) and amplified for 35 cycles with 0.1 μg of BC-1 DNA as a template. PCR product was intially cloned into PCR-Script (Stratagene, La Jolla, CA) from which an EcoRV insert was then cloned into the pMET7 expression vector [Y. Takebe *et al.*, *Mol. Cell. Biol.* **8**, 466 (1988); kindly provided by J. Culpepper] and transfected by means of DEAE-dextran plus chloroquine into COS7 cells (CRL-1651, American Type Culture Collection, Rockville, MD). The EcoRV insert was also cloned into the pMET7 vector in the reverse orientation (6-LIv) relative to the SRα promoter as a negative control, with orientation and sequence fidelity of both constructs confirmed by bidirectional sequencing by means of dye-primer chemistry on an ABI 377 sequenator (Applied Biosystems Inc., Foster City, CA).
22. Serum-free COS7 supernatants (15 ml) were concentrated to 1.5 ml by ultrafiltration with a Centriplus 10 filter (Amicon, Beverly, MA) and 100 μl of supernatant concentrate or 1 μg of rhuIL-6 (R&D Systems, Minneapolis, MN) was loaded per each lane in Laemmeli buffer. For cell lysate immunoblotting, exponential phase cells with and without TPA (20 ng/ml) induction for 48 hours were pelleted and 100 μg of whole protein cell protein solubilized in Laemmeli buffer was loaded per lane, separated by electrophoresis on a 15% SDS-polyacrylamide gel and immunoblotted and developed by means of standard conditions (*8*) with either rabbit antipeptide antibody (1:100-1:1000 dilution) or anti-huIL-6 (1 μg per milliliter; R&D Systems, Minneapolis, MN).
23. M. M. Schwarze and R. G. Hawley, *Cancer Res.* **55**, 2262 (1995). B9 mouse plasmacytoma cell line (provided by M. Yellin, Columbia University) was maintained in Iscove's Modified Dulbecco's Medium (IMDM) (Gibco, Gaithersburg, MD), 10% fetal bovine serum (FBS), 1% penicillin + streptomycin, 1% glutamine, 50 μM B-mercaptoethanol, and 10 ng per milliliter of rhuIL-6 (R&D Systems, Minneapolis, MN). ^{3}H-thymidine uptake was used to measure B9 proliferation in response to huIL-6 or recombinant supernatants according to standard protocols (courtesy A. Flemming, R&D Systems, Minneapolis, MN). Briefly, serial 1:3 dilutions of huIL-6 or Centriplus 10 concentrated recombinant supernatants were incubated with 2×10^4 cells per well in a 96-well plate for 24 hours at 37°C with 10 μl of thymidine stock solution (50 μl of 1 mCi/ml ^{3}H-thymidine in 1 ml IMDM) added to each well during the final 4 hours of incubation. Cells were harvested and incorporation of ^{3}H-thymidine determined with a liquid scintillation counter. Each data point is the average of six determinations with standard deviations shown.
24. Immunostaining was performed with the avidin-biotin complex (ABC) method after deparaffinization of tissues and quenching for 30 min with 0.03% H_2O_2 in PBS by standard immunohistochemical protocols available from authors. The primary antibody was applied at a dilution of 1:1250 after blocking with 10% normal goat serum, 1% BSA, 0.5% Tween 20 and developed with diamino-benzidine (DAB) chromogen. Amino ethyl carbazole (AEC) or Vector Red staining was also used to better discriminate double-labeled cells, with Fast Blue counterstaining for some surface antigens. Cell antigens were examined with the following antibodies: CD68 (1:800, from clone Kim 6 kindly provided by G. Cattoretti and visualized by fluorescein-rhodamine double-labeling), epithelial membrane antigen (EMA, 1:500, Dako, Carpinteria, CA), CD3 (1:200, Dako), CD20 (1:200, Dako), OPD4 (1:100, Dako), CD34 (1:15, Dako), CD45 (1:400, from clone 9.4 kindly provided by G. Cattoretti), L26 (1:100, Immunotech, Westbrook, ME) and Leu22 (1:100, Becton-Dickinson, San Jose, CA) on tissues prepared according to manufacturer's instructions. Specific vIL-6 colocalization was only found with CD34 and CD45 in KS lesions, EMA in PEL, and CD20 and CD45 in lymph node tissues. The authors thank L. Ward for extensive help in immunohistochemistry preparations.
25. Immunohistochemical vIL-6 localization was performed on exponential phase BCP-1 cells with or without 48-hour TPA incubation after embedding in 1% agar in saline. The percentages of positive cells were determined from cell counts of three random high power microscopic fields per slide. Lower percentages of BCP-1 cells stain positively for vIL-6 after TPA treatment possibly reflecting cell lysis and death from lytic virus replication induction by TPA. The vIL-6 immunostaining of both cells and tissues was confirmed by neutralization after overnight incubation of antisera with vIL-6 synthetic peptides (0.1 μg/ml) at 4°C and with preimmune rabbit antisera run in parallel to the postimmune immunostaining. No specific staining was seen after either peptide neutralization or use of preimmune sera.
26. W. Zhong, H. Wang, B. Herndier, D. Ganem, *Proc. Natl. Acad. Sci. U.S.A.* **93**, 6641 (1996).
27. F. Cocchi *et al.*, *Science* **270**, 1811 (1995); T. Dragic *et al.*, *Nature* **381**, 667 (1996); H. Deng *et al.*, *ibid.*, p. 661.
28. CCR5 (kindly provided by Patrick Gray, ICOS Corp.) was cloned into pRcCMV vector (Invitrogen) and both forward and reverse orientations of the vMIP-I gene were cloned into pMET7 after PCR amplification

with the primer pairs described (*16*). CCR5 alone and with the forward construct (vMIP-I), the reverse construct (I-PIMv), and empty pMET7 vector were transfected into CCC/CD4 cells [A. McKnight, P. R. Clapham, R. A. Weiss, *Virology* **201**, 8 (1994)] by means of Lipofectamine (Gibco). After 48 hours, media was removed from the transfected cells and 1000 $TCID_{50}$ of SF162, M23, or ROD/B virus culture stock was added. Cells were washed four times after 4 hours of virus incubation and grown in DMEM with 5% FBS for 72 hours before immunostaining for HIV-1 p24 or HIV-2 gp105. Each condition was replicated three to four times with medians and error bars representing the standard deviations expressed as percentages of the foci formed in the presence of CCR5 alone.
29. G. Simmons *et al.*, *J. Virol.* **70**, 8355 (1996); P. R. Clapham, A. McKnight, R. A. Weiss, *J. Virol.* **66**, 3531 (1992).
30. P. M. Murphy, *Infect. Agents Dis.* **3**, 137 (1994); T. G. Senkevich *et al.*, *Science* **273**, 813 (1996); J.-C. Albrecht *et al.*, *J. Virol.* **66**, 5047 (1992); J. L. Gao and P. M. Murphy, *J. Biol. Chem.* **269**, 28539 (1994); M. S. Chee *et al.*, *Curr. Top. Microbiol. Immunol.* **154**, 125 (1990); R. F. Massung *et al.*, *Virology* **201**, 215 (1994).
31. R. Sarid, T. Sato, R. Bohenzky, J. Russo, Y. Chang, in preparation; E. Cesarman *et al.*, *J. Virol.* **70**, 8218 (1996); Y. Chang *et al.*, *Nature* **382**, 410 (1996); R. Sarid, P. S. Moore, Y. Chang, unpublished observation.
32. M. L. Cleary, S. D. Smith, J. Sklar, *Cell* **47**, 19 (1986); I. Palmero *et al.*, *Oncogene* **8**, 1049 (1993); C. Larcher *et al.*, *Eur. J. Immunol.* **25**, 1713 (1995); M. Birkenbach, K. Josefsen, R. Yalamanchili, G. Lenoir, E. Kieff, *J. Virol.* **67**, 2209 (1993).
33. G. Tosato, J. Tanner, K. D. Jones, M. Revel, S. E. Pike, *J. Virol.* **64**, 3033 (1990).
34. Y. Shen and T. E. Shenk, *Curr. Opin. Gen. Dev.* **5**, 105 (1995); K. H. Vousden, *Sem. Cancer Biol.* **6**, 109 (1995); L. J. Appleman and A. B. Frey, *Int. J. Cancer* **63**, 576 (1995).
35. A. Lichtenstein, Y. Tu, C. Fady, R. Vescio, J. Berenson, *Cell. Immunol.* **162**, 248 (1995).
36. C. Holzinger *et al.*, *Immunol. Lett.* **35**, 109 (1993).
37. A. Lafeuillade, G. Kaplanski, T. Allegre, J. P. de Jaureguiberry, *J. AIDS Hum. Retrovirol.* **12**, 95 (1996); T. Cohen, D. Nahari, L. W. Cerem, G. Neufeld, B.-Z. Levi, *J. Biol. Chem.* **271**, 736 (1996).
38. G. Scala *et al.*, *J. Exp. Med.* **172**, 61 (1990).
39. H. Harada *et al.*, *Science* **259**, 971 (1993).
40. A. M. Hardy, *J. AIDS* **4**, 386 (1991); G. F. Lemp, S. F. Payne, D. Neal, T. Temelso, G. W. Rutherford, *J. Am. Med. Assoc.* **263**, 402 (1990); R. Rothenberg *et al.*, *N. Engl. J. Med.* **317**, 1297 (1987); L. P. Jacobson *et al.*, *Am. J. Epidemiol.* **138**, 953 (1993); J. D. Lundgren, M. Melbye, C. Pederson, P. S. Rosenberg, J. Gerstoft, *ibid.* **141**, 652 (1995).
41. Abbreviations for the amino acid residues are: A, Ala; C, Cys; D, Asp; E, Glu; F, Phe; G, Gly; H, His; I, Ile; K, Lys; L, Leu; M, Met; N, Asn; P, Pro; Q, Gln; R, Arg; S, Ser; T, Thr; V, Val; W, Trp; and Y, Tyr.
42. The authors thank R. A. Bohenzky, J. Russo, and I. A. Edelman for collaborative work on genomic sequencing of KSHV; G. Simmons for help with HIV inhibition experiments, J. Strauchen for PEL tissue sections; Y.-Z. Cao, S. Silverstein, J. Luban and C. Parravicini for helpful discussions; R. Sarid, J. P. Parry, M. Yan, W. Zheng and A.-E. Thlick for technical assistance; and M. Davis and D. Holland for help in preparing the manuscript. Supported by NIH NCI grant CA67391, an award from the James S. McDonnell Foundation, the Cancer Research Campaign, and the Mercury Phoenix Trust.

30 August 1996; accepted 23 October 1996

A Role for Endothelial NO Synthase in LTP Revealed by Adenovirus-Mediated Inhibition and Rescue

David B. Kantor, Markus Lanzrein, S. Jennifer Stary, Gisela M. Sandoval, W. Bryan Smith, Brian M. Sullivan, Norman Davidson, Erin M. Schuman*

Pharmacological studies support the idea that nitric oxide (NO) serves as a retrograde messenger during long-term potentiation (LTP) in area CA1 of the hippocampus. Mice with a defective form of the gene for neuronal NO synthase (nNOS), however, exhibit normal LTP. The myristoyl protein endothelial NOS (eNOS) is present in the dendrites of CA1 neurons. Recombinant adenovirus vectors containing either a truncated eNOS (a putative dominant negative) or an eNOS fused to a transmembrane protein were used to demonstrate that membrane-targeted eNOS is required for LTP. The membrane localization of eNOS may optimally position the enzyme both to respond to Ca^{2+} influx and to release NO into the extracellular space during LTP induction.

Long-term potentiation, a form of synaptic plasticity, can be inhibited by agents that interfere with the activity of NO synthase (NOS), which suggests that NO serves as a retrograde messenger during some forms of LTP (*1*–*6*). Hippocampal slices from homozygous transgenic mice lacking neuronal NOS (nNOS), however, exhibited normal LTP (*7*). The LTP in slices from these mutant mice was still susceptible to inhibition by broad-spectrum NOS inhibitors, which suggests that another NOS isoform may participate in LTP. In fact, a residual NOS activity was detected in the hippocampus of these mice (*8*), perhaps resulting from endothelial NOS (eNOS) in CA1 neurons (*7*, *9*). Thus, eNOS may be the isoform of NOS that participates in LTP induction.

Division of Biology 216-76, California Institute of Technology, Pasadena, CA 91125, USA.

*To whom correspondence should be addressed. E-mail: schumane@cco.caltech.edu

Endothelial NOS is myristoylated and associated with membrane fractions (*10*–*12*). We assessed the subcellular localization of eNOS by examining the distribution of fluorescence in Chinese hamster ovary (CHO) cells transfected with a cDNA encoding a fusion protein composed of eNOS and green fluorescent protein (*13*, *14*) [the fluorescent protein used was Green Lantern (GL)] (*15*, *16*). Control cells transfected with GL alone exhibited a diffuse fluorescent signal throughout the cytoplasm and the nucleus (Fig. 1A), whereas the eNOS-GL fusion protein was localized in the plasmalemma membrane and intracellular membrane compartments (Fig. 1B) (*17*).

We examined the role of eNOS in LTP by combining pharmacological agents with recombinant adenovirus vectors that were designed to manipulate eNOS function. In control experiments, individual rat hippocampal slices were injected in the CA1 cell body region with an adenovirus vector containing *lac*Z (Ad-lacZ) (*15*, *18*). We examined synaptic transmission and plasticity at the Schaffer-collateral CA1 neuron synapses with conventional extracellular recording techniques (*19*). Control slices infected with Ad-lacZ exhibited staining for β-galactosidase (β-Gal) throughout the pyramidal cell layer and in processes extending into the stratum radiatum (SR) and stratum oriens (SO) within 4 to 8 hours of injection (Fig. 2A) (*18*); single pyramidal neurons expressing β-Gal were readily identified (Fig. 2B). Synaptic transmission (24 to 36 hours after infection) in Ad-lacZ–infected slices was indistinguishable from slices injected with control saline that were maintained for equivalent periods of time (Fig. 2C). In addition, short- and long-term synaptic plasticity, including post-tetanic potentiation (PTP), paired-pulse facilitation (PPF), and LTP, were normal (Fig. 2, C and D) [100-ms interstimulus interval (ISI) PPF, mean percent of the first field excitatory postsynaptic potential (fEPSP) slope ± SEM: saline, 126.2 ± 4.9% (n = 4); Ad-lacZ, 133.5 ± 4.5% (n = 4), not significant (NS); maximum PTP, mean percent of baseline ± SEM: saline, 345.0 ± 37.7% (n = 6); Ad-lacZ, 359.7 ± 21.9% (n = 6), NS; LTP, mean percent of baseline ± SEM: saline, 193.3 ± 25.3% (n = 6); Ad-lacZ, 184.7 ± 7.7% (n = 6), NS].

To address the role of eNOS in LTP, we constructed an adenovirus vector containing a truncated eNOS (Ad-TeNOS) (*15*). The truncated eNOS lacks catalytic activity yet retains the NH_2-terminal sequence required for myristoylation and may be a dominant negative inhibitor of eNOS function, presumably because it can heterodimerize with wild-type eNOS (*20*). Co-transfection of CHO cells with eNOS-GL